THE JOURNAL OF BIOLOGICAL CHEMISTRY VOL. 287, NO. 46, pp. 38835–38844, November 9, 2012


# MinD and MinE Interact with Anionic Phospholipids and Regulate Division Plane Formation in *Escherichia coli*[*][S]

Received for publication, August 3, 2012, and in revised form, September 22, 2012 Published, JBC Papers in Press, September 25, 2012, DOI 10.1074/jbc.M112.407817

**Lars D. Renner**[‡1] **and Douglas B. Weibel**[‡§2]

*From the Departments of* [‡]*Biochemistry and* [§]*Biomedical Engineering, University of Wisconsin, Madison, Wisconsin 53706*

**Background:** Understanding the bacterial division machinery is essential to decoding cellular physiology.
**Results:** The cell division proteins MinD/MinE bind tightly to anionic lipids, which reduces ATPase activity.
**Conclusion:** MinD and MinE interact preferably with anionic lipids that are positioned at the cell pole.
**Significance:** These results provide insight into a mechanism that regulates bacterial cell division and may present a useful target for antimicrobial development.

**The Min proteins (MinC, MinD, and MinE) form a pole-to-pole oscillator that controls the spatial assembly of the division machinery in *Escherichia coli* cells. Previous studies identified that interactions of MinD with phospholipids positioned the Min machinery at the membrane. We extend these studies by measuring the affinity, kinetics, and ATPase activity of *E. coli* MinD, MinE, and MinDE binding to supported lipid bilayers containing varying compositions of anionic phospholipids. Using quartz crystal microbalance measurements, we found that the binding affinity ($K_d$) for the interaction of recombinant *E. coli* MinD and MinE with lipid bilayers increased with increasing concentration of the anionic phospholipids phosphatidylglycerol and cardiolipin. The $K_d$ for MinD (1.8 $\mu$M) in the presence of ATP was smaller than for MinE (12.1 $\mu$M) binding to membranes consisting of 95:5 phosphatidylcholine/cardiolipin. The simultaneous binding of MinD and MinE to membranes revealed that increasing the concentration of anionic phospholipid stimulates the initial rate of adsorption ($k_{on}$). The ATPase activity of MinD decreased in the presence of anionic phospholipids. These results indicate that anionic lipids, which are concentrated at the poles, increase the retention of MinD and MinE and explain its dwell time at this region of bacterial cells. These studies provide insight into interactions between MinD and MinE and between these proteins and membranes that are relevant to understanding the process of bacterial cell division, in which the interaction of proteins and membranes is essential.**

A hallmark of cell division is the establishment of the division plane. *Escherichia coli* cell division involves the spatial and temporal localization of a protein ensemble that demarcates the mid-cell (1, 2). In *E. coli*, the Min proteins, consisting of MinC, MinD, and MinE, form a pole-to-pole oscillator that regulates the assembly of the division plane (3). The oscillation of MinD and MinE creates a temporal gradient of MinC, which is an antagonist of FtsZ and prevents its assembly into the Z-ring and the subsequent organization of the division machinery. Several models have explored the influence of cell geometry and membrane composition on the placement of the cell division machinery (4–6). Despite the apparent simplicity of this oscillatory system, an understanding of the interactions between the Min proteins and their association with the membrane is still emerging (7–9).

MinD is a central component of this mechanism. MinD dimerizes in an ATP-dependent manner and binds the membrane via its amphipathic C-terminal helix (10, 11). MinD has a preference for interacting with anionic phospholipids, such as phosphatidylglycerol (PG)[3] and 1′,3′-bis(1,2-dioleoyl-*sn*-glycero-3-phospho)-*sn*-glycerol (cardiolipin; CL), which represent ~25 and ~5% of phospholipids in the *E. coli* membrane (12), respectively (9, 13). The poles of *E. coli* cells are reportedly enriched in CL due to its response to membrane curvature (6, 14–16). It has been hypothesized that the positioning of MinD *in vivo* may be influenced by the curvature of the pole and the interaction between proteins and polar, anionic lipid-rich regions of the membrane (2, 8, 10).

Both MinC and MinE bind to MinD close to its dimerization interface (17). The binding of a dimer of MinE to MinCD has been reported to trigger the release of MinC followed by stimulating the ATPase activity of MinD and its dissociation from the membrane (18, 19). In one current model of the Min system, MinD binds to the membrane as a dimer and functions as the spatial determinant for recruiting MinC. MinE migrates outward from the mid-cell toward the pole, where it binds MinD, triggers its ATPase activity, and releases MinC and subsequently MinD into the cytoplasm (17). MinD and MinC diffuse through the cytoplasm, MinD binds to the membrane at the other polar region of the cell, and the process repeats (17). Reac-

* This work was supported by an Alfred P. Sloan Foundation fellowship (to D. B. W.), the Kinship Foundation Searle Scholarship (to D. B. W.), a Deutsche Forschungsgemeinschaft fellowship (to L. D. R.), and National Science Foundation Grant DMR-0520527.
[S] This article contains supplemental Figs. S1–S10.
[1] Present address: Technische Universität Dresden, Institute for Materials Sciences and Max Bergmann Center for Biomaterials, 01062 Dresden, Germany.
[2] To whom correspondence should be addressed: Depts. of Biochemistry and Biomedical Engineering, University of Wisconsin, 433 Babcock Dr., Madison, WI 53706. Tel.: 608-890-1342; E-mail: weibel@biochem.wisc.edu.

[3] The abbreviations used are: PG, phosphatidylglycerol (1,2-dioleoyl-*sn*-glycero-3-phospho-(1′-*rac*-glycerol) or DOPG); PC, phosphatidylcholine (1,2-dioleoyl-*sn*-glycero-3-phosphocholine or DOPC); CL, cardiolipin; SLB, supported bilayer; QCM-D, quartz crystal microbalance with dissipation monitoring.

tion diffusion models can recapitulate the oscillation of the Min proteins *in silico* (20, 21). Remarkably, a component of the Min oscillation can be reconstituted by the addition of recombinant MinD and MinE to supported lipid bilayers *in vitro* (18, 22, 23).

In addition to measurements of MinCDE dynamics *in vivo* and *in vitro*, several studies have addressed the binding of MinD and MinE to phospholipid membranes with varying anionic composition (7–9, 24, 25). For example, Mileykovskaya *et al.* (9) demonstrated that MinD has a preference for binding to anionic phospholipids and that division plane formation may be regulated by the composition of the membrane. Hsieh *et al.* (7) demonstrated that MinE binds to bacterial cell membranes directly via its N-terminal domain. Interestingly, this region of the protein is proposed to stimulate the ATPase activity of MinD. A triple mutant of MinE (R10G/K11E/K12E) no longer bound to phospholipid bilayers and yet retained its ability to stimulate the ATPase activity of MinD (7). The triple MinE mutant prevented the localization and oscillation of the Min system *in vivo* (7) and the oscillation of recombinant MinD on a supported bilayer (SLB) *in vitro* (22). These studies suggest that a direct interaction between MinE and membranes may contribute to the localization of MinDE and its oscillation *in vivo*. The determination of values for the affinity and kinetics of the binding of MinD, MinE, and MinDE to the membrane may facilitate an understanding of the mechanism of the Min proteins *in vivo*.

In this paper, we use a quartz crystal microbalance with dissipation monitoring (QCM-D) to measure the binding affinity ($K_d$), adsorption rate ($k_{on}$), desorption rate ($k_{off}$), and ATPase activity for MinD, MinE, and MinDE to SLBs and liposomes with a user-defined composition. SLBs provide a versatile experimental platform for mimicking the properties of cell membranes (18, 23, 26). Our results complement and extend the foundational studies of Mileykovskaya *et al.* (9), which measured the equilibrium binding of MinD to liposomes of various compositions.

The application of QCM-D to measure $K_d$ provides advantages over liposome and sedimentation assays because it enables the monitoring of proteins interacting with membranes in real time. Fitting QCM-D binding curves made it possible for us to extract the kinetics of protein-lipid binding. We found that the concentration of the anionic lipids PG and CL had a substantial effect on the binding affinity and rate of MinD and MinE to membranes and demonstrated that electrostatic interactions play a dominant role in the phospholipid binding properties of these proteins. Further, the presence of anionic phospholipids decreased the ATPase activity of MinD, which influences the rate of MinC dissociation from MinD. These results provide insight into the interaction of MinD and MinE and their association with membranes and suggest a mechanism by which the proteins are excluded from the mid-cell, where their presence inhibits the formation of the division plane.

## EXPERIMENTAL PROCEDURES

*Lipid and Liposome Preparation*—1,2-Dioleoyl-*sn*-glycero-3-phosphocholine (DOPC; we refer to this lipid as PC), 1,2-dioleoyl-*sn*-glycero-3-phospho-(1′-*rac*-glycerol) (DOPG; we refer to this lipid as PG), and CL were from Avanti Polar Lipids Inc. (Alabaster, AL). We dissolved mixtures of lipids in chloroform and evaporated them under a stream of argon. For these studies, we used mixtures of PC/PG at a molar ratio of 100:0, 90:10, 80:20, 70:30, and 50:50 and PC/CL at a molar ratio of 97.5:2.5, 95:5, 92.5:7.5, and 90:10. We dried lipid mixtures under vacuum overnight before use. We hydrated dried lipid mixtures in 10 mM Tris buffer (Sigma-Aldrich), pH 8.0, containing 100 mM NaCl (Sigma-Aldrich) and 5 mM $CaCl_2$ (Sigma-Aldrich) to a final lipid concentration of 5 mg/ml and homogenized the samples using four cycles of freezing in liquid nitrogen followed by thawing in a sonication bath (Branson 2510). We extruded lipid mixtures 21 times through a polycarbonate membrane filter containing 50-nm diameter pores (Avanti Polar Lipids Inc.) following the procedure of Mayer *et al.* (27). We stored lipid solutions sealed at 4 °C under an atmosphere of argon and used the samples within 1 week after preparation.

*QCM-D Measurements*—We used a QCM-D E1 and E4 (QSense AB, Biolin Scientific AB, Gothenburg, Sweden) to measure the binding of MinD and MinE to SLBs. In QCM-D experiments, the frequency ($\Delta f$) and dissipation ($\Delta D$) changes of a quartz crystal are extrapolated from measuring the piezoelectric properties of the crystal (28). The frequency change of a quartz crystal can be directly correlated to changes in mass and reflects the adsorption of material on the surface. The dissipation is attributed to dissipative energy losses of the material deposited on the oscillating crystal surface and can be used to analyze the viscoelastic properties of the attached molecules.

Quartz crystals (QSense AB, Biolin Scientific AB, Gothenburg, Sweden) were coated with a 50-nm-thick layer of silicon dioxide by chemical vapor deposition (GeSiM GmbH, Dresden, Germany). Before use, we oxidized the crystals in a solution consisting of a 1:1:5 volumetric ratio of concentrated ammonium hydroxide (Sigma-Aldrich), 30% hydrogen peroxide (Fisher), and ultrapure water (Millipore, Billerica, MA) at 70 °C. We oxidized crystals in an oxygen plasma chamber (Harrick Plasma, Ithaca, NY) for 2 min at high radio frequency, immediately placed them into the measurement chamber, and covered them with ultrapure water (Millipore, Billerica, MA).

A representative example of a QCM-D measurement is shown in Fig. 1. We initiated measurements by exchanging water in the flow cell with 10 mM Tris buffer, pH 8.0, until we observed a drift of the signal less than 0.1 Hz/min. Subsequently, we introduced a suspension of fresh liposomes (0.2 mg/ml) to the crystal and observed the characteristic profile of SLB formation (29, 30). After 5 min, we rinsed the sensor surface with 10 mM Tris buffer, pH 8.0, added solutions of MinD or MinE at a range of concentrations (0.168–54.2 $\mu$M) to the SLB surface, and measured binding (Fig. 1). MinD or MinE were adsorbed for 5–10 min or until a stable base line was observed, and the quartz crystals containing adsorbed protein were rinsed with 10 mM Tris buffer, pH 8.0. MinD or MinE was almost completely removed from the SLB surfaces during rinsing with Tris buffer. We performed multiple protein adsorption and desorption cycles on each SLB. We measured the binding of MinD to SLBs in the absence or presence of ATP. For experiments with ATP, we added 2.5 mM ATP and 10 mM $MgCl_2$ to

the protein solution. All measurements were performed at 24 °C.

We analyzed the data by extracting the maximum frequency changes and plotting the frequency *versus* the protein concentration. The corresponding binding curves were fit to the Hill equation (Equation 1) to calculate binding coefficients,

$$\Gamma(c) = \frac{c^n}{K_d + c^n} \qquad \text{(Eq. 1)}$$

where Γ is the surface coverage (binding of MinD/MinE to the SLB), $c$ is the concentration of MinD/MinE, $K_d$ is the equilibrium dissociation constant, and $n$ is the Hill coefficient that denotes the cooperativity of binding. Briefly, a Hill coefficient with $n > 1$ indicates positive cooperativity, $n < 1$ indicates negative cooperativity, and $n = 1$ indicates non-cooperativity.

Additionally, we analyzed the kinetics of each individual binding event. We fit the plots to a second order exponential decay function and extrapolated to determine the adsorption ($k_{on}$) and desorption rates ($k_{off}$).

*Preparation of Recombinant MinD and MinE*—We produced and purified MinD (pI 5.1) and MinE (pI 5.3) by modifying the protocol reported by Ivanov and Mizuuchi (23). We transformed *E. coli* BL21 cells with the plasmids encoding MinD X05, coding for proteins translationally fused to an N-terminal $His_6$ tag, and MinE X09, coding for fusions to a C-terminal $His_6$ tag, and plated the transformants as described by Ivanov and Mizuuchi (23). We picked individual colonies and grew them overnight in Luria-Bertani medium to saturation (30 ml supplemented with 50 μg/ml ampicillin). We inoculated a 2-liter culture of Luria-Bertani medium with the overnight culture, adjusted the density to an absorbance of 0.05 (λ = 600 nm), and grew the culture at 37 °C to an absorbance of 0.6 (λ = 600 nm). At this absorbance, we induced protein expression by adding 1 mM isopropyl 1-thio-β-D-galactopyranoside, 0.2% L-arabinose, and 200 μl of antifoam agent 204 (Sigma-Aldrich) to the culture medium, transferred the culture flasks to a refrigerated incubator, and grew them overnight at 16 °C.

The next day, we incubated the culture on ice for 10 min. We centrifuged cells at 10,000 × *g* for 15 min at 4 °C and resuspended them in ice-cold lysis buffer consisting of 50 mM $NaH_2PO_4$, pH 7.5, 300 mM NaCl, 10 mM imidazole, and freshly added 10 mM β-mercaptoethanol, protease inhibitor PMSF (0.02 mg/ml of buffer), and 0.2 mM Mg-ADP. All of these reagents were from Sigma-Aldrich. We cooled the cell suspension on ice for 10 min, lysed the cells using a French press, and clarified the crude cell lysate by centrifugation at 10,000 × *g* for 30 min at 4 °C. We collected the supernatant in a 50-ml centrifuge tube (C1060, Denville Scientific Inc., Metuchen, NJ) and stored it on ice. 2 ml of $Ni^{2+}$-Sepharose resin (GE Healthcare) was added to the cell suspension. The $Ni^{2+}$-Sepharose resin was equilibrated with imidazole buffer consisting of 50 mM $NaH_2PO_4$, pH 7.5, 300 mM NaCl, 20 mM imidazole, 10% glycerol, protease inhibitor PMSF (0.02 mg/ml of buffer), and 0.1 mM EDTA. The suspension was incubated on a rocking shaker at 4 °C for 2–3 h. We poured the resin into a column and washed it three times with imidazole buffer containing increasing concentrations of imidazole (20, 50, and 70 mM). We eluted the protein fraction containing the $His_6$ tag from the resin using elution buffer consisting of 50 mM $NaH_2PO_4$, pH 7.5, 300 mM NaCl, 300 mM imidazole, 10% glycerol, 0.1 mM EDTA, protease inhibitor PMSF (0.02 mg/ml of buffer), and 0.2 mM ADP.

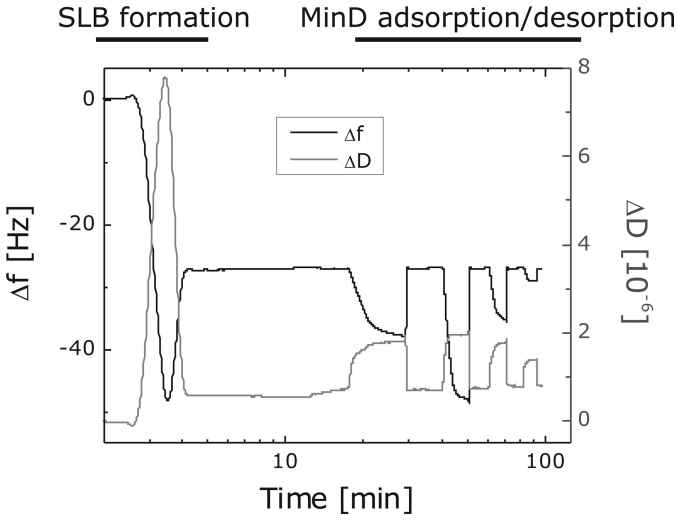


FIGURE 1. **Example of a characteristic QCM-D data set depicting SLB formation and MinD binding.** An SLB consisting of 90:10 PC/PG was formed on a silicon dioxide-coated surface of a quartz crystal from a suspension of liposomes. In this experiment, we added MinD (0.168–1.68 μM) to the SLB and measured the frequency (Δ*f*, *black line*) and dissipation (Δ*D*, *gray line*) changes. This plot demonstrates that MinD can be completely desorbed from the SLB, and subsequent MinD binding measurements can be performed on the same bilayer. Each peak indicates the injection of a new aliquot of MinD. The MinD solutions contained 10 mM Tris buffer, 2.5 mM ATP, and 10 mM $MgCl_2$. Measurements were performed at 24 °C.

We further concentrated the protein fractions through Vivaspin molecular weight cut-off membranes (GE Healthcare) to purify MinD (30 kDa) and MinE (10 kDa) (supplemental Fig. S10). In the last step, we exchanged the purified and concentrated protein solutions into storage buffer consisting of 50 mM HEPES, pH 7.25, 150 mM KCl, 10% glycerol, 0.1 mM EDTA, and 0.2 mM ADP (for MinD) using a PD10 desalting column (GE Healthcare). We aliquoted the protein fractions into Eppendorf tubes, froze them in liquid nitrogen, and stored the aliquots at −80 °C.

*MinD ATPase Activity Assay*—We used an ATP/NADH-coupled assay to measure ATPase activity that is based on the regeneration of ATP (A2383, Sigma-Aldrich) by the coupled oxidation of NADH (N8129, Sigma-Aldrich). Each cycle of ATP hydrolysis was followed by regeneration of ATP by phosphoenolpyruvate (860077, Sigma-Aldrich) and pyruvate kinase. Conversion of pyruvate to lactate by lactate dehydrogenase resulted in the oxidation of NADH to NAD. We used a TECAN plate reader to measure the NADH absorbance at λ = 340 and 380 nm of 150-μl reaction volumes in the wells of a 96-well plate at 24 °C. For these assays, we used 2 μM MinD and 2 μM MinE in the presence of 2.5 mM ATP and 0.2 mg/ml liposome solutions.

## RESULTS

*Binding of MinD to SLBs Consisting of PC, PG, and CL*—An example of the formation of a SLB measured by QCM-D is shown in Fig. 1. Measurements of the formation of SLBs on silicon dioxide surfaces by QCM-D have been described in

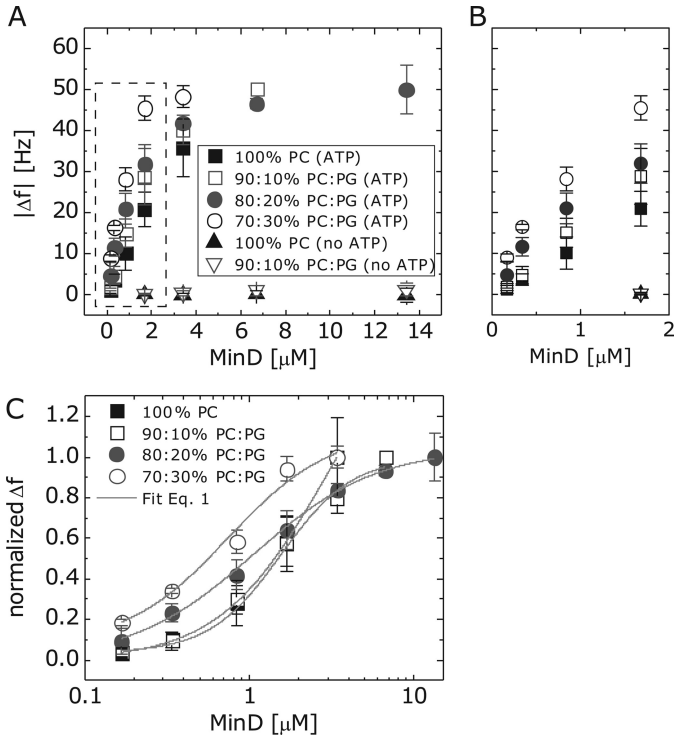


FIGURE 2. **MinD adsorption to supported lipid bilayers.** *A*, frequency change measured for the binding of MinD (0.168–13.4 μM) to SLBs containing PC and varying amounts of PG (values indicate mol %). *B*, *magnified view* illustrating the data points close to the origin. *C*, plot of the normalized Δ*f*, data from *A* that were fit using adsorption isotherms to determine the $K_d$ for MinD binding (Equation 1, $R^2 > 0.98$). *Error bars*, S.D. of at least three independent measurements.

**TABLE 1**

**Binding constants $K_d$ for MinD and MinE calculated by fitting the binding curves to Equation 1**

All fits for MinE resulted in a Hill coefficient of $n = 1$, indicating non-cooperative binding. ND, not determined.

| Lipid mixtures | MinD $K_d$ | MinD $n$ | MinE $K_d$ |
|---|---|---|---|
| | μM | | μM |
| PC 100 | 3.01 | 1.34 | ND |
| PC/CL (97.5:2.5) | 1.7 | 1.7 | 21.5 |
| PC/CL (95:5) | 1.8 | 1.84 | 12.1 |
| PC/PG (90:10) | 1.42 | 1.42 | 9.2 |
| PC/PG (80:20) | 1.16 | 1.15 | 5.9 |
| PC/PG (70:30) | 0.74 | 1.22 | 1.1 |

detail previously (29–31). Briefly, the model for SLB formation involves liposomes adsorbing on hydrophilic silicon dioxide surfaces, accumulating until a critical coverage is established, and fusing into large liposomes. As the size of liposomes increases, they become unstable, rupture, and form a planar SLB. QCM-D measurements of planar SLB formation on silicon dioxide display a characteristic frequency change (Δ*f*) of ~−25 to −30 Hz and a dissipation change (Δ*D*) of ~0.1–1 × $10^{-6}$. SLBs on planar surfaces are intrinsically stable due to the favorable balance of interfacial forces, including electrostatic repulsion and attraction between charged lipid head groups and the substrate surface (32).

We formed SLBs with a range of concentrations of PC/PG and PC/CL on quartz crystals coated with a layer of silicon dioxide and measured the interaction of recombinant MinD or MinE at different concentrations. We observed that the binding of both proteins was predominantly reversible, which enabled us to repeat measurements on individual SLBs. The adsorption of MinD to SLBs consisting of 100% PC and PC/PG in the absence of ATP did not produce a significant increase in Δ*f*, even at MinD concentrations of >2 μM (Fig. 2 and supplemental Fig. S1).

The addition of 2.5 mM ATP to the MinD solution resulted in the binding of protein to SLBs for all of the lipid compositions used in this study, including 100% PC. We observed that the binding of MinD to SLBs was non-linear and strongly dependent on protein concentration at all lipid compositions (Fig. 2). Increasing the concentration of MinD enhanced Δ*f* and Δ*D* (Fig. 1) and increased the amount of adsorbed MinD. Above a threshold concentration of MinD (between 4–6 μM), we observed that the binding of MinD became saturated. The onset of saturation was dependent on the lipid composition of the SLB. We observed a significant difference in the binding affinity of MinD to SLBs upon introducing PG to the lipid mixture. Increasing the concentration of PG in the SLB enhanced the binding affinity of MinD (Fig. 2). Increasing the concentration of PG to 30% decreased the $K_d$ of MinD by a factor of 4 compared with SLBs consisting of 100% PC (Table 1). Despite extensive experimentation, we were unable to form SLBs containing PC with a concentration of PG of >30% (supplemental Fig. S2 shows an example for 50:50 PC/PG). We fit the binding curves to Equation 1 and found a correlation between the decrease in $K_d$ with increasing PG concentration (Fig. 2*B* and Table 1). Interestingly, the composition of lipids had less of an effect on Δ*D* than on Δ*f*. Fig. 1 shows Δ*f* and Δ*D* for MinD binding to a SLB of PC/PG 90:10; between the first and second adsorption steps, Δ*D* was negligible, whereas Δ*f* nearly doubled. The nearly constant value of Δ*D* suggests that monolayers of protein are assembling on SLBs of varying composition.

We studied the interaction of CL with MinD. CL is an anionic phospholipid with an intrinsic curvature of 0.45–1.33 $nm^{-1}$ (33, 34) that is widely found in bacterial membranes, where it destabilizes bilayers (12). We recently studied the relationship between negative membrane curvature, CL microdomain localization, and the positioning of MinD in *E. coli* spheroplasts (15). We found that CL microdomains and MinD co-localized in spheroplast membranes, which supported the hypothesis that CL may be a spatial determinant for the localization and function of this protein *in vivo*. To connect these observations to quantitative biophysical measurements, we studied the adsorption of MinD to PC/CL bilayers using QCM-D. We were able to form SLBs with concentrations of CL ≤5%, which is biologically relevant because the concentration of CL in *E. coli* membranes approaches this value at stages of cell growth (35). We were unable to form SLBs containing CL concentrations of >5% and hypothesize that the intrinsic curvature of CL precludes formation of stable, planar SLBs (supplemental Fig. S3).

We found no significant difference between the $K_d$ for 95:5 and 97.5:2.5 PC/CL (Fig. 3 and Table 1). For SLBs containing CL, the $K_d$ was comparable with the binding of MinD to 90:10 PC/PG (Table 1). Fitting the data to the Hill equation yielded values of $n$ for 97.5:2.5 PC/CL (1.7), 95:5 PC/CL (1.35), 90:10 PC/PG (1.4), 80:20 PC/PG (1.17), and 70:30 PC/PG (1.14). These values indicate that the binding of MinD to the SLB is

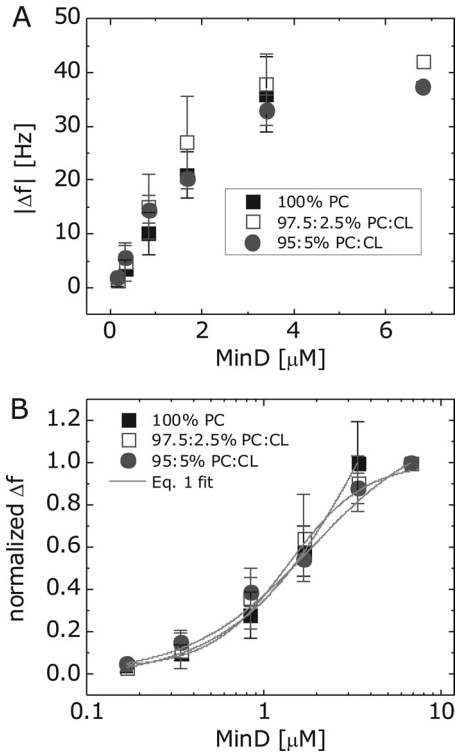


FIGURE 3. **MinD adsorption to SLBs containing CL.** *A*, frequency change measured for the binding of MinD (0.168–6.8 $\mu$M) to SLBs containing PC and varying amounts of CL (values indicate mol %). We were unable to form stable SLBs with concentrations of CL > 5%. *B*, plot of the normalized $\Delta f$ data from *A* that was fit using adsorption isotherms to determine the $K_D$ for MinD binding (Equation 1, $R^2 > 0.98$). *Error bars*, S.D. of at least three independent measurements.

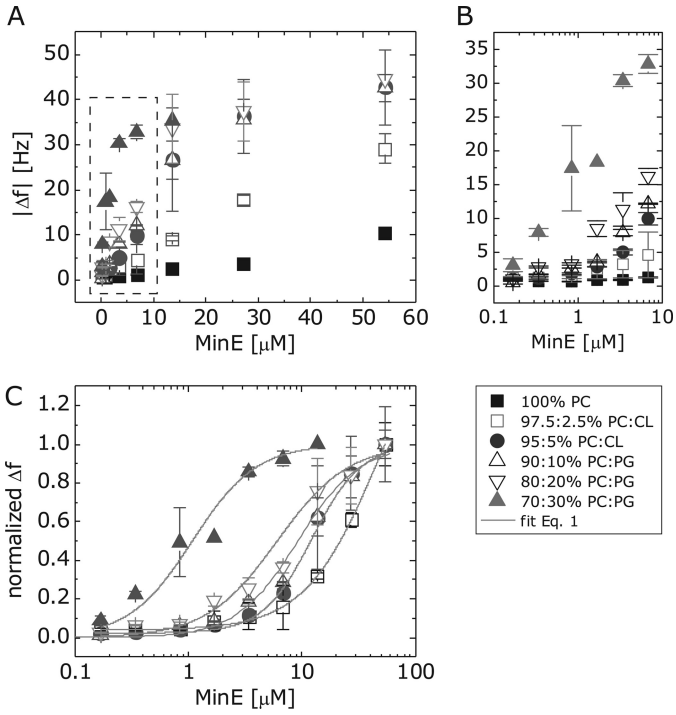


FIGURE 4. **MinE adsorption to SLBs.** *A*, plot depicting the binding of MinE (0.168–54.2 $\mu$M) to SLBs consisting of PC and PG or CL. *B*, *magnified view* illustrating the data points close to the origin. *C*, plot of the normalized $\Delta f$ data from *A* that was fit using adsorption isotherms to determine the $K_D$ for MinE binding (Equation 1, $R^2 > 0.98$). The legend for *C* also applies to *A* and *B*. *Error bars*, S.D. of at least three independent measurements.

cooperative and depends on the composition of anionic phospholipids.

*Binding of MinE to SLBs Consisting of PC/PG and PC/CL*—We studied the binding of MinE to SLBs with varying compositions of PC/PG and PC/CL. We observed that only small amounts of MinE adsorbed to SLBs consisting of 100% PC and 97.5:2.5 PC/CL; binding was predominantly reversible over the concentration range we investigated (Fig. 4*A* and supplemental Fig. S5). The qualitative binding of MinD and MinE to these SLBs is similar. However, at higher concentrations of MinE (≥12.1 $\mu$M), we observed partially irreversible binding of protein to the SLB (supplemental Fig. S6). Increasing the concentration of CL to 5% decreased the $K_d$ of MinE to 12.1 $\mu$M (Table 1). Unable to prepare stable SLBs with a CL concentration above 5%, we could not study the effect of higher CL concentrations on MinE binding (supplemental Fig. S3).

The incorporation of PG into SLBs had a significant effect on the $K_d$ of MinE to membranes. Increasing the concentration of PG to 10% resulted in a decrease in $K_d$ (9.2 $\mu$M) that was comparable with SLBs containing 95:5 PC/CL (12.1 $\mu$M) (Fig. 4 and Table 1). We increased the concentration of PG to 20 and 30% and observed a further decrease in the $K_d$ for MinE to SLBs from 5.9 to 1.1 $\mu$M (Fig. 4 and Table 1), suggesting that MinE preferentially binds to SLBs that have a high concentration of anionic phospholipids. Qualitatively, the relationship between increasing PG concentration and a decrease in the $K_d$ for MinE to SLBs is comparable with our observations with MinD. However, the actual $K_d$ of MinE to SLBs containing PG is at least 5 times weaker than for MinD (Table 1). At the highest concentration of PG that we studied (30%), the $K_d$ for MinD and MinE to SLBs only differs by a factor of 1.3 (0.74 *versus* 1.1 $\mu$M). We observed that the saturation of MinE binding to SLBs was achieved at a much higher protein concentration (>27 $\mu$M) than for MinD (4–6 $\mu$M).

*Simultaneous Binding of MinD and MinE to SLBs*—As the Min oscillation consists of the interaction of MinD and MinE at membranes, we studied the simultaneous binding of MinD and MinE to SLBs to mimic the interaction of the Min proteins with the membrane *in vitro*. We measured the co-adsorption of an equimolar ratio of MinD and MinE (1.68 $\mu$M) on SLBs (Fig. 5). For comparison, the concentrations of MinD and MinE in the cell are 0.8 and 1.2 $\mu$M, respectively (36, 37). The adsorption of MinD and MinE correlated to the concentration of anionic lipids in the SLB (Fig. 5 and supplemental Fig. S7). The kinetic profiles of protein binding were influenced by the concentration of anionic lipids. In contrast to the kinetics of the individual adsorption of MinD or MinE, we observed three distinct phases for the co-adsorption of both proteins (supplemental Fig. S8): 1) rapid adsorption; 2) intermediate desorption and displacement; and 3) slow desorption during rinsing of the crystal in buffer (Fig. 5). For the adsorption of either MinD or MinE on SLBs, we were only able to distinguish two phases: 1) protein adsorption until the SLB was saturated; and 2) the desorption of protein during the rinsing of the crystal with buffer (Fig. 5 and supplemental Fig. S8).

*MinD ATPase Activity*—To extend our understanding of the influence of membranes on MinDE, we measured how this pro-

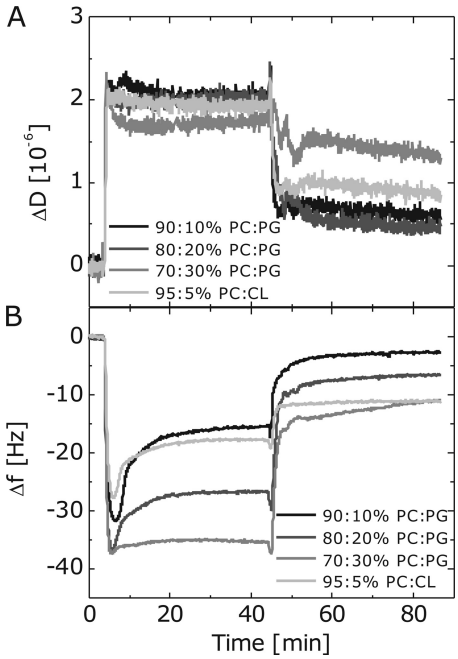


FIGURE 5. **Kinetics of simultaneous binding of MinD and MinE.** Simultaneous binding of MinD and MinE to SLBs consisting of PC/PG and PC/CL. *A*, plot depicting the Δ*D* accompanying the simultaneous binding of MinD and MinE to SLBs with varying ratios of PC/PG and PC/CL. *B*, plot depicting the Δ*f* accompanying the simultaneous binding of MinD and MinE to SLBs with varying ratios of PC/PG and PC/CL. The legend for *B* also applies to *A*. The MinDE mixtures contained 10 mM Tris buffer, 2.5 mM ATP, and 10 mM $MgCl_2$. Measurements were performed at 24 °C.

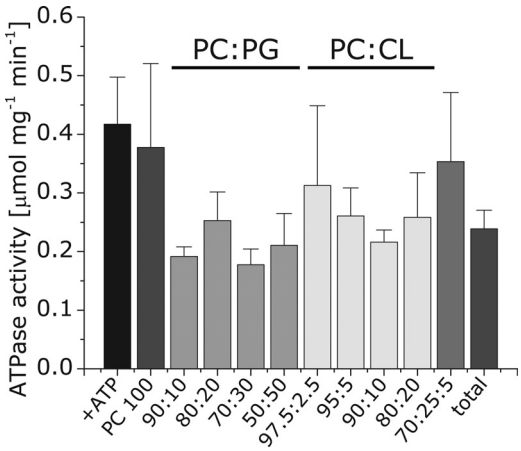


FIGURE 6. **MinD ATPase activity assay.** The results of a coupled enzymatic ATPase activity for MinD. We performed the assay using MinD (2 μM) in the presence of MinE (2 μM) and different liposome compositions. *Error bars*, S.D.

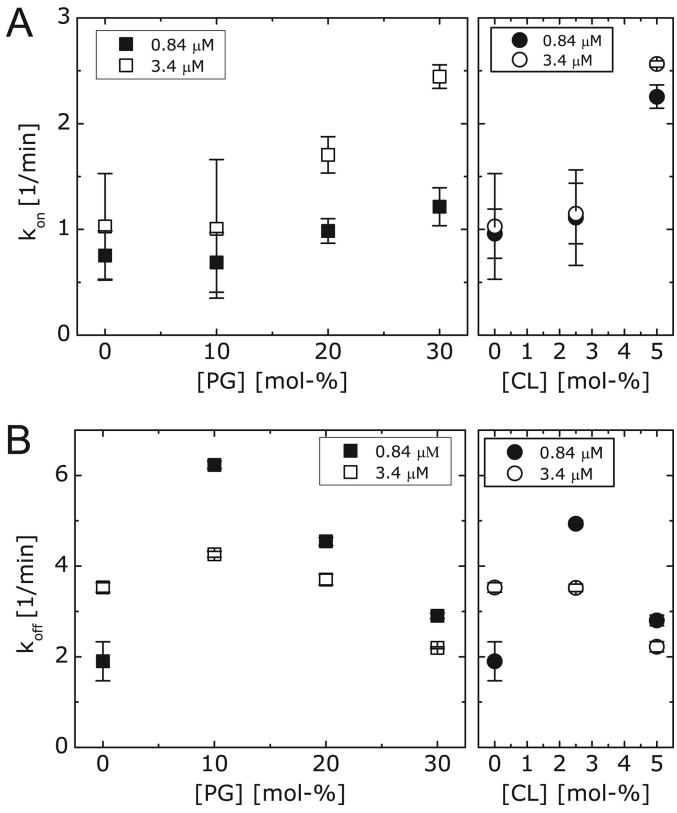


FIGURE 7. **Rates of $k_{on}$ and $k_{off}$ for MinD binding to SLBs.** Plots depict the $k_{on}$ (*A*) and $k_{off}$ (*B*) for MinD (0.84 or 3.4 μM) binding to SLB bilayers containing varying ratios of PC/PG and PC/CL. *Inset values* indicate the concentration of MinD. *Error bars*, S.D.

tein-lipid interaction influences the ATPase activity of MinD *in vitro* using a coupled enzyme assay in the presence of MinE. We observed a decrease in the ATPase activity of MinD in the presence of liposomes containing negatively charged lipids, in contrast to liposomes containing 100% PC (Fig. 6). The ATPase activity of MinD was lower for all of the PC/PG concentrations we tested, compared with 100% PC, and no differences between the concentrations were apparent. In contrast, the ATPase activity of MinD in the presence of PC/CL liposomes decreased with increasing concentrations of CL. This ATPase activity of MinD was comparable with its activity in the presence of *E. coli* total lipid mixture.

## DISCUSSION

*MinD Binding to SLBs*—The binding of MinD to SLBs in the presence of ATP was strongly dependent on the lipid composition. Our experiments confirmed previous measurements by Mileykovskaya *et al.* (9) that measured the binding affinity of MinD to liposomes of different lipid composition. We expanded these measurements by using QCM-D, which enabled us to extract kinetic data from binding curves at different concentrations of MinD, PG, and CL (Fig. 7). The $k_{on}$ for MinD binding to bilayers followed a general trend in which the rate increased with increasing concentrations of anionic lipids (Fig. 7*A*). The values of $k_{on}$ for MinD binding to 100% PC and 97.5:2.5 PC/CL were approximately identical (Fig. 7*A*). The trend for $k_{off}$ was reversed, and higher concentrations of anionic lipids resulted in the slower desorption of MinD from SLBs (Fig. 7*B*); the $k_{off}$ for 100% PC did not follow the trend, which may be due to its zwitterionic distribution of charges. MinD clearly has an increased affinity for PG and CL.

Binding of ATP to MinD exposes its C-terminal membrane-targeting sequence (38, 39). The membrane-targeting sequence consists of a positively charged, hydrophobic region that is important for binding to membranes and enhances the electrostatic interaction of MinD with anionic phospholipids (17). At comparable concentrations of anionic phospholipids, we found no preference for MinD binding to CL *versus* PG. Although we were unable to increase the concentration of CL in SLBs above

5%, the highest concentration of CL found in *E. coli* membranes has been reported to be only ~8%, which is close to the highest values we used (35). The $K_d$ for MinD binding to 5% CL (1.8 $\mu$M) was similar to the binding of MinD to 10% PG (1.42 $\mu$M). These data may reflect the anionic character presented by CL (two phosphate groups instead of one for PG) and a larger hydrophobic region for binding of the membrane-targeting sequence than for PG. If this hypothesis is correct, PG and CL may similarly facilitate the binding of proteins to membranes, albeit at different stoichiometries.

We calculated the protein layer thickness from the maximum changes in frequency using the Sauerbrey equation, which correlates $\Delta f$ to mass changes (40). The results are summarized in supplemental Fig. S4. At the highest concentrations of MinD in our experiments (13.4 $\mu$M), we found that the maximum thickness of the protein layer was ~7.5 nm. Taking into consideration the sensitivity of QCM-D and the estimated 6.4-nm length scale for the MinD dimer crystal structure (Protein Data Bank code 3Q9L) (17), the thickness derived from the calculation is compatible with the formation of a monolayer of protein. We conclude that MinD does not form a multilayer at the range of MinD concentrations used in our experiments. The formation of a MinD monolayer supports the hypothesis that the binding of MinD dimers at the SLB interface is regulated by its interaction with the membrane. The thickness of the protein layers was consistent at all lipid compositions that we studied.

*MinE Binding to SLBs*—The MinE adsorption measurements support a model in which its interaction with membranes is required for the correct function of the cell division machinery (7). The binding of MinE to 70:30 PC/PG ($K_d$ = 1.1 $\mu$M) was comparable with MinD binding to 80:20 PC/PG ($K_d$ = 1.16 $\mu$M). In contrast to the interaction of MinD with membranes, $k_{on}$ and $k_{off}$ for MinE binding to SLBs is not clearly correlated to lipid composition (Fig. 8). In general, the differences in $k_{on}$ are almost identical for all PG concentrations we tested (Fig. 8*A*). The $k_{off}$ values for MinE on all lipid compositions appear to decrease with increasing MinE concentrations (Fig. 8*B*). The $k_{off}$ values are almost identical for MinE concentrations of ≥6.8 $\mu$M, except for an outlier at 97.5:2.5 PC/CL.

One interpretation of these results is that MinE has a strong interaction potential with high concentrations of anionic phospholipids. Park *et al.* (17) recently identified a membrane-binding $\alpha$-helix in MinE that only interacts with the membrane upon binding to MinD. However, we found that MinE binds to SLBs in the absence of MinD. The strongest interaction we observed with MinE was its binding to a 70:30 PC/PG lipid mixture, which is the closest lipid composition to *E. coli* membranes that we studied. The interaction of MinE may be crucial for the proper functioning of the division machinery because the binding of MinE to the membrane stimulates MinD ATPase activity, the release of MinC and MinD from the membrane, and the oscillation of the Min system between the two polar regions to ensure the placement of the FtsZ ring at midcell (9, 17).

The rates of $k_{on}$ and $k_{off}$ for MinE did not follow a clear trend. The $k_{on}$ rates were high for the two CL concentrations we studied (2.5 and 5%) and decreased with an increase in MinE concentration (Fig. 8*A*). The $k_{on}$ for MinE to PG-containing SLBs was slow and increased with increasing concentrations of MinE. These results suggest that increasing the CL concentration increased the rate of MinE binding to SLBs and a preference for binding to membranes containing PG. This interaction may be important at the cell poles, where MinE is required to displace MinD and stimulate the oscillation of the Min system to the opposing cell pole.

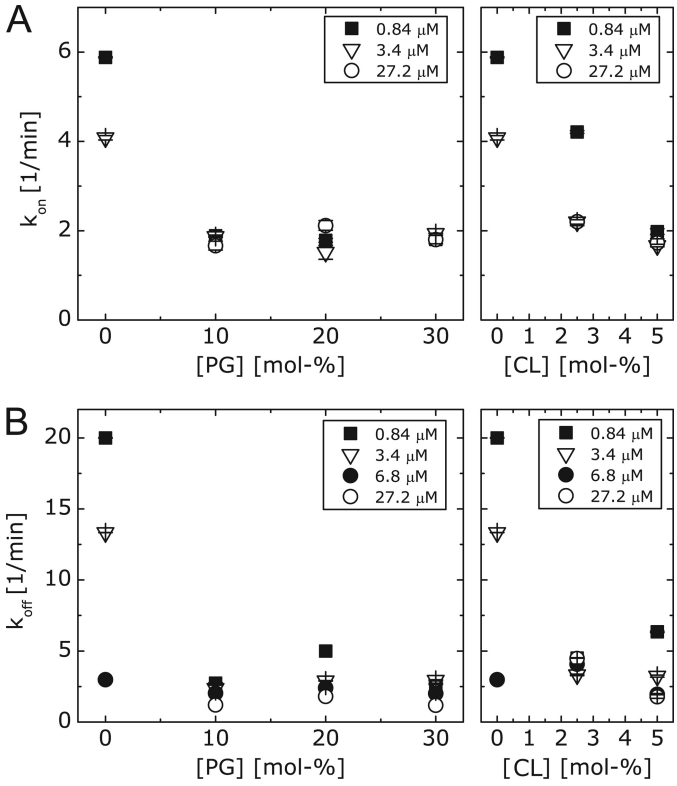


FIGURE 8. **Rates of $k_{on}$ and $k_{off}$ for MinE binding to SLBs.** Plots depict the $k_{on}$ (*A*) and $k_{off}$ (*B*) for MinE (0.84, 3.4, or 27.2 $\mu$M) binding to SLB bilayers containing varying ratios of PC/PG and PC/CL. *Inset values* indicate the concentration of MinE. Each data point represents an average of at least three measurements; *error bars* are included and represent S.D.

We calculated the MinE protein layer thickness from the maximum $\Delta f$ (supplemental Fig. S4) and found it to be between ~5.4 and 6.5 nm thick. These values are close to the estimated length of the MinE dimer based on the crystal structure (~4.5 nm) (Protein Data Bank code 3R9J) (17). Our measurements suggest that MinE dimers form a monolayer at the SLB interface.

*Simultaneous Binding of MinD and MinE*—The kinetics for the simultaneous binding and desorption of MinD and MinE to SLBs were significantly different from the kinetics for the individual proteins. We observed three stages occurring in the simultaneous binding assays (supplemental Fig. S8). In the first stage, MinD and MinE bound SLBs at approximately the same rate, as evidenced by similar values of $k_{on}$ (Table 2). In the presence of both MinD and MinE, the observed $k_{on}$ was significantly higher and suggests that MinE may stimulate the binding of MinD, or *vice versa*. The magnitude of $\Delta f$ that we observe indicates the adsorption of both MinD and MinE in monolayers to SLBs (confirming the results of monolayer formation for each individual protein).

**TABLE 2**

**Comparison of the rate constants $k_{on}$ and $k_{off}$ for the binding of MinD and MinE and the simultaneous binding of MinDE at a concentration of 1.68 $\mu$M**

The simultaneous binding of MinDE occurred in three stages: 1) protein binding characterized by $k_{on}$; 2) an intermediate stage with two rates ($k_{fast}$ and $k_{slow}$); and 3) protein desorption characterized by $k_{off}$.

| Lipid mixtures | MinD | | MinE | | MinDE | | | |
|---|---|---|---|---|---|---|---|---|
| | $k_{on}$ | $k_{off}$ | $k_{on}$ | $k_{off}$ | $k_{on}$ | $k_{fast}$ | $k_{slow}$ | $k_{off}$ |
| | $min^{-1}$ | | $min^{-1}$ | | $min^{-1}$ | | | |
| PC/CL (95:5) | 2.25 | 2.75 | 1.3 | 3.4 | 2.12 | 0.99 | 0.14 | 1.72 |
| PC/PG (90:10) | 0.59 | 6.22 | 1.83 | 2.72 | 2.38 | 0.55 | 0.11 | 3.22 |
| PC/PG (80:20) | 1.18 | 4.53 | 1.45 | 3.76 | 2.56 | 1.33 | 0.17 | 1.19 |
| PC/PG (70:30) | 1.2 | 3 | 1.94 | 2.62 | 2.94 | 2.44 | 0.13 | 1.14 |

In the second stage, we observed a reversal in the direction of the frequency shifts. One explanation for this behavior may be the onset of MinD displacement by MinE at the SLB interface. The initial displacement occurs rapidly (indicated by $k_{fast}$) and over time reaches equilibrium (indicated by $k_{slow}$) (Table 2). These observations may indicate the process of detachment and displacement of MinD from the membrane by MinE; the data support the two fascinating examples of reconstituted Min systems *in vitro* (18, 23). Although it is unclear from our *in vitro* measurements whether MinE is membrane-associated or proximal to the membrane during this step (*i.e.* the direct interaction of MinE with MinD without initial membrane binding), the $K_d$ for the interaction of MinE with the SLB suggests that either scenario may be possible. A current model is that the binding of MinE to the membrane is stimulated by the presence of MinD (17). The displacement of MinD reaches an equilibrium that is defined by a constant $\Delta f$. We hypothesize that the equilibrium is defined by constant MinD and MinE displacement and proceeds until most of the ATP in solution is hydrolyzed. This result can be compared with the reappearing waves for the *in vitro* Min system (18, 22, 23). Alternatively, the equilibrium we observe may indicate that all free ATP has been consumed, although this scenario is unlikely, given the short time scale of the experiment.

In the third and last stage, we introduced buffer into the flow cell and observed the rapid desorption of the MinD and MinE mixture. This process is comparable with stage 2 for the binding and desorption of individual proteins. Interestingly, there is no indication of substantial changes in the viscoelastic properties of membrane-bound proteins during stages 1–3. Although we expected that characteristic frequency changes would produce similar dissipation profiles, we observed that the changes in $\Delta D$ were subtle, which agrees with the observations of monolayers for the individual proteins (Fig. 5). The overall kinetics strongly depend on the lipid composition.

We repeated the simultaneous binding of MinDE (1.68 $\mu$M) to SLBs three times and observed the same characteristic (Fig. 7). We also observed comparable results for 1:1 $\mu$M and 1:2 $\mu$M stoichiometries of MinD/MinE (supplemental Fig. S9). However, a ratio of 0.8:1.2 $\mu$M MinD/MinE did not produce a similar kinetic profile (supplemental Fig. S9); these values reflect the reported concentrations of MinD and MinE *in vivo* (36, 37). It is unclear why the MinD/MinE stoichiometry of 1:1 works well in this assay. Increasing the concentration of MinE by a factor of 5 (to 5 $\mu$M) produced different results (supplemental Fig. S9). We attribute this result to the enhanced rate of displacement of MinD by the high concentration of MinE, which led to pronounced simultaneous binding and displacement of the proteins. Our observation that MinD is rapidly displaced at a high concentration of MinE is supported by the observation of an increase in the oscillation frequency of MinD at high MinE concentrations (41). Although it would have been ideal to bind MinD to the SLB and then to chase it with MinE to measure protein dissociation, we found that MinD dissociated as we introduced buffer into the flow cell, which unfortunately made these experiments impossible.

*ATPase Activity*—Our results indicate a lower conversion rate of ATP by MinD in the presence of negatively charged membranes and MinE. This observation may be related to the binding efficiency of MinD to anionic phospholipids affecting the accessibility of MinE and its influence on the structure of MinD and its rate of ATP hydrolysis. However, we also observed the ATPase activity of MinD in the absence of MinE. Shih *et al.* (42) observed that the assembly and disassembly of polar zones of MinD still occur in the absence of MinE rings, which confirms that the ATPase activity may be unrelated to the presence of MinE. Hence, it appears that the ATPase activity of MinD is independent of the simultaneous binding of MinD and MinE to liposomes in our experiments.

Our observation of the tight binding of MinD to CL and its suppression of ATPase activity upon binding may explain the dwell time of MinD at the cell poles during observations of oscillations *in vivo*, where CL appears to be enriched in the membranes (14, 15) (*i.e.* enhanced binding to the polar regions of membranes may decrease the local displacement of MinD by MinE). Decreased $k_{off}$ rates for MinD from the SLB with higher anionic concentrations also correspond to low ATPase activity.

Hu *et al.* (43) demonstrated that the rate of ATP hydrolysis by MinD is independent of the concentration of MinE; however, the lag phase depends on MinE concentration. The observed desorption behavior of MinD can be interpreted by a model in which the detachment of MinD by stimulation of its ATPase activity by MinE is not a required step.

Various mechanisms have been proposed for organizing Min protein function in rod-shaped cells (4, 44–46). It is unclear how a mechanism based upon phospholipid organization may coordinate the spatial oscillation of the Min system in round-shaped cells. However, small deformations of the shape of these cells lead to the realignment and oscillation of the Min proteins (4, 44, 45). The model that arises from our observations is supported by recent computational studies that treated MinD as a polymer strand and MinE as an inducer of its ATPase activity (47). The polar bias of polymerized MinD dimers can be explained by tension created through MinD polymers that

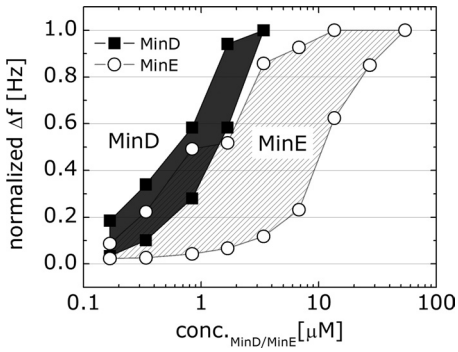


FIGURE 9. **MinD and MinE adsorption behavior.** A plot depicts Δ*f versus* the concentration of MinD and MinE. The *top data curves* for MinD and MinE represent the binding of proteins to SLBs consisting of 70:30 PC/PG. The *bottom data curves* represent binding to SLBs consisting of 90:10 PC/PG. We connected the two data sets for each protein to map out the region of binding for MinD and MinE. The Δ*f* for MinD and MinE binding overlap at protein concentrations of $<1.68$ $\mu$M.

induces membrane curvature by the binding of the amphipathic helix. The increase in tension may induce local membrane curvature and increase MinD attachment due to an increase in its accessibility (47, 48). Although MinD is accessible to MinE in model membranes that contain no or low amounts of anionic lipids, increasing concentrations of CL and PG may deform the local shape of the membrane and increase MinD binding. This step in turn decreases the probability of the detachment of MinD and its ATPase activity in the presence of MinE because it impedes the binding of MinE to the membrane. Binding of MinE to the membrane does not necessarily require the presence of negatively charged lipids; however, the retention times of both proteins at the poles may be related to the presence of anionic lipids at this region of the membrane or the proposed curvature mechanism (47). We were unable to detect membrane deformations using QCM-D, which leaves the hypothesis of the role of CL in membrane bending unanswered. In summary, our results suggest that negatively charged lipids play a role in cell division site selection.

In this study, we studied the binding of the bacterial division proteins MinD and MinE to SLBs consisting of varying compositions of phospholipids. We observed that both MinD and MinE have a high affinity to SLBs, as evidenced by the values of $K_d$, that correlates to the concentration of anionic phospholipids in the membrane (Fig. 9). Whereas MinD binds to both neutral and anionic SLBs (9), MinE is less promiscuous and selective for binding to anionic SLBs. MinD showed no apparent preference for binding to CL using the two PC/CL SLB compositions from which we were able to create stable SLBs. However, these experiments are not sufficient to rule out a concentration dependence on MinD binding to CL. In contrast, the binding of MinE to membranes is dependent on CL concentration. At the highest concentration of PG that we studied (30%), the $K_d$ for MinD and MinE differs by a factor of 1.3, which is close to the experimental error of our measurements. Our inability to create SLBs containing more than 5% CL prevented our studies of how incremental changes in CL affect MinD and MinE binding to SLBs. Taking into consideration previous studies describing the role of MinE membrane adsorption (7, 8), our data support a mechanism for the preferential association of MinDE at the poles, where the concentration of anionic lipids is high; these results also indicate that the dissociation from membrane-bound MinD and MinE at this region of the cell should be slow. Our measurements of the ATPase activity of MinD in the presence of liposomes corroborate this mechanism because high concentrations of anionic lipids reduce the ATP hydrolysis rate of MinD. Finally, overlaying our measurements on the reported distribution of CL and PG in the cell supports a mechanism in which MinD and MinE bind the membrane and may preferentially dwell at the poles, in contrast to localization along the cylindrical region of the cell, and is consistent with a recent analysis of the composition and concentration of proteins in polar vesicles (49). The interaction of MinD and MinE with anionic phospholipids is emerging as an important mechanism for the spatial positioning of the division inhibitor machinery.

*Acknowledgments—We thank the Pedersen laboratory for access to the QCM-D, George Whitesides for loaning us a Q-Sense D300, and Kurt Jacobsen for technical assistance.*

## REFERENCES

1. de Boer, P. A., Crossley, R. E., and Rothfield, L. I. (1989) A division inhibitor and a topological specificity factor coded for by the minicell locus determine proper placement of the division septum in *E. coli*. *Cell* **56,** 641–649
2. Hu, Z., and Lutkenhaus, J. (1999) Topological regulation of cell division in *Escherichia coli* involves rapid pole to pole oscillation of the division inhibitor MinC under the control of MinD and MinE. *Mol. Microbiol.* **34,** 82–90
3. Bramkamp, M., and van Baarle, S. (2009) Division site selection in rod-shaped bacteria. *Curr. Opin. Microbiol.* **12,** 683–688
4. Huang, K. C., and Wingreen, N. S. (2004) Min protein oscillations in round bacteria. *Phys. Biol.* **1,** 229–235
5. Fange, D., and Elf, J. (2006) Noise-induced Min phenotypes in *E. coli*. *PLoS Comput. Biol.* **2,** e80
6. Varma, A., Huang, K. C., and Young, K. D. (2008) The Min system as a general cell geometry detection mechanism. Branch lengths in Y-shaped *Escherichia coli* cells affect Min oscillation patterns and division dynamics. *J. Bacteriol.* **190,** 2106–2117
7. Hsieh, C. W., Lin, T. Y., Lai, H. M., Lin, C. C., Hsieh, T. S., and Shih, Y. L. (2010) Direct MinE-membrane interaction contributes to the proper localization of MinDE in *E. coli*. *Mol. Microbiol.* **75,** 499–512
8. Shih, Y. L., Huang, K. F., Lai, H. M., Liao, J. H., Lee, C. S., Chang, C. M., Mak, H. M., Hsieh, C. W., and Lin, C. C. (2011) The N-terminal amphipathic helix of the topological specificity factor MinE is associated with shaping membrane curvature. *PLoS One* **6,** e21425
9. Mileykovskaya, E., Fishov, I., Fu, X., Corbin, B. D., Margolin, W., and Dowhan, W. (2003) Effects of phospholipid composition on MinD-membrane interactions *in vitro* and *in vivo*. *J. Biol. Chem.* **278,** 22193–22198
10. Hu, Z., and Lutkenhaus, J. (2001) Topological regulation of cell division in *E. coli*. Spatiotemporal oscillation of MinD requires stimulation of its ATPase by MinE and phospholipid. *Mol. Cell* **7,** 1337–1343
11. Wu, W., Park, K. T., Holyoak, T., and Lutkenhaus, J. (2011) Determination of the structure of the MinD-ATP complex reveals the orientation of MinD on the membrane and the relative location of the binding sites for MinE and MinC. *Mol. Microbiol.* **79,** 1515–1528
12. Cronan, J. E. (2003) Bacterial membrane lipids. Where do we stand? *Annu. Rev. Microbiol.* **57,** 203–224
13. Barák, I., Muchová, K., Wilkinson, A. J., O'Toole, P. J., and Pavlendová, N. (2008) Lipid spirals in *Bacillus subtilis* and their role in cell division. *Mol. Microbiol.* **68,** 1315–1327
14. Mileykovskaya, E., and Dowhan, W. (2000) Visualization of phospholipid

domains in *Escherichia coli* by using the cardiolipin-specific fluorescent dye 10-*N*-nonyl acridine orange. *J. Bacteriol.* **182,** 1172–1175
15. Renner, L. D., and Weibel, D. B. (2011) Cardiolipin microdomains localize to negatively curved regions of *Escherichia coli* membranes. *Proc. Natl. Acad. Sci. U.S.A.* **108,** 6264–6269
16. Koppelman, C. M., Den Blaauwen, T., Duursma, M. C., Heeren, R. M., and Nanninga, N. (2001) *Escherichia coli* minicell membranes are enriched in cardiolipin. *J. Bacteriol.* **183,** 6144–6147
17. Park, K. T., Wu, W., Battaile, K. P., Lovell, S., Holyoak, T., and Lutkenhaus, J. (2011) The Min oscillator uses MinD-dependent conformational changes in MinE to spatially regulate cytokinesis. *Cell* **146,** 396–407
18. Loose, M., Fischer-Friedrich, E., Herold, C., Kruse, K., and Schwille, P. (2011) Min protein patterns emerge from rapid rebinding and membrane interaction of MinE. *Nat. Struct. Mol. Biol.* **18,** 577–583
19. Lackner, L. L., Raskin, D. M., and de Boer, P. A. (2003) ATP-dependent interactions between *Escherichia coli* Min proteins and the phospholipid membrane *in vitro*. *J. Bacteriol.* **185,** 735–749
20. Huang, K. C., Meir, Y., and Wingreen, N. S. (2003) Dynamic structures in *Escherichia coli*. Spontaneous formation of MinE rings and MinD polar zones. *Proc. Natl. Acad. Sci. U.S.A.* **100,** 12724–12728
21. Kruse, K., Howard, M., and Margolin, W. (2007) An experimentalist's guide to computational modeling of the Min system. *Mol. Microbiol.* **63,** 1279–1284
22. Loose, M., Fischer-Friedrich, E., Ries, J., Kruse, K., and Schwille, P. (2008) Spatial regulators for bacterial cell division self-organize into surface waves *in vitro*. *Science* **320,** 789–792
23. Ivanov, V., and Mizuuchi, K. (2010) Multiple modes of interconverting dynamic pattern formation by bacterial cell division proteins. *Proc. Natl. Acad. Sci. U.S.A.* **107,** 8071–8078
24. Mazor, S., Regev, T., Mileykovskaya, E., Margolin, W., Dowhan, W., and Fishov, I. (2008) Mutual effects of MinD-membrane interaction. I. Changes in the membrane properties induced by MinD binding. *Biochim. Biophys. Acta* **1778,** 2496–2504
25. Mazor, S., Regev, T., Mileykovskaya, E., Margolin, W., Dowhan, W., and Fishov, I. (2008) Mutual effects of MinD-membrane interaction. II. Domain structure of the membrane enhances MinD binding. *Biochim. Biophys. Acta* **1778,** 2505–2511
26. Sackmann, E. (1996) Supported membranes. Scientific and practical applications. *Science* **271,** 43–48
27. Mayer, L. D., Hope, M. J., and Cullis, P. R. (1986) Vesicles of variable sizes produced by a rapid extrusion procedure. *Biochim. Biophys. Acta* **858,** 161–168
28. Rodahl, M., Höök, F., Krozer, A., and Brzezinski, P. (1995) Quartz crystal microbalance set up for frequency and Q-factor measurements in gaseous and liquids environments. *Rev. Sci. Instrum.* **66,** 3924–3930
29. Keller, C. A., Glasmästar, K., Zhdanov, V. P., and Kasemo, B. (2000) Formation of supported membranes from vesicles. *Phys. Rev. Lett.* **84,** 5443–5446
30. Keller, C. A., and Kasemo, B. (1998) Surface-specific kinetics of lipid vesicle adsorption measured with a quartz crystal microbalance. *Biophys. J.* **75,** 1397–1402
31. Johnson, J. M., Ha, T., Chu, S., and Boxer, S. G. (2002) Early steps of supported bilayer formation probed by single vesicle fluorescence assays. *Biophys. J.* **83,** 3371–3379
32. Israelachvili, J. (2005) Differences between nonspecific and bio-specific, and between equilibrium and non-equilibrium, interactions in biological systems. *Q. Rev. Biophys.* **38,** 331–337
33. Huang, K. C., and Ramamurthi, K. S. (2010) Macromolecules that prefer their membranes curvy. *Mol. Microbiol.* **76,** 822–832
34. Rand, R. P., and Sengupta, S. (1972) Cardiolipin forms hexagonal structures with divalent cations. *Biochim. Biophys. Acta* **255,** 484–492
35. Romantsov, T., Helbig, S., Culham, D. E., Gill, C., Stalker, L., and Wood, J. M. (2007) Cardiolipin promotes polar localization of osmosensory transporter ProP in *Escherichia coli*. *Mol. Microbiol.* **64,** 1455–1465
36. de Boer, P. A., Crossley, R. E., Hand, A. R., and Rothfield, L. I. (1991) The MinD protein is a membrane ATPase required for the correct placement of the *Escherichia coli* division site. *EMBO J.* **10,** 4371–4380
37. Szeto, T. H., Rowland, S. L., and King, G. F. (2001) The dimerization function of MinC resides in a structurally autonomous C-terminal domain. *J. Bacteriol.* **183,** 6684–6687
38. Szeto, T. H., Rowland, S. L., Habrukowich, C. L., and King, G. F. (2003) The MinD membrane targeting sequence is a transplantable lipid-binding helix. *J. Biol. Chem.* **278,** 40050–40056
39. Szeto, T. H., Rowland, S. L., Rothfield, L. I., and King, G. F. (2002) Membrane localization of MinD is mediated by a C-terminal motif that is conserved across eubacteria, archaea, and chloroplasts. *Proc. Natl. Acad. Sci. U.S.A.* **99,** 15693–15698
40. Sauerbrey, G. (1959) Verwendung von Schwingquarzen zur Wägung dünner Schichten und zur Mikrowägung. *Z. Physik A Hadrons Nuclei* **155,** 206–222
41. Raskin, D. M., and de Boer, P. A. (1999) Rapid pole-to-pole oscillation of a protein required for directing division to the middle of *Escherichia coli*. *Proc. Natl. Acad. Sci. U.S.A.* **96,** 4971–4976
42. Shih, Y. L., Fu, X., King, G. F., Le, T., and Rothfield, L. (2002) Division site placement in *E. coli*. Mutations that prevent formation of the MinE ring lead to loss of the normal midcell arrest of growth of polar MinD membrane domains. *EMBO J.* **21,** 3347–3357
43. Hu, Z., Gogol, E. P., and Lutkenhaus, J. (2002) Dynamic assembly of MinD on phospholipid vesicles regulated by ATP and MinE. *Proc. Natl. Acad. Sci. U.S.A.* **99,** 6761–6766
44. Corbin, B. D., Yu, X. C., and Margolin, W. (2002) Exploring intracellular space. Function of the Min system in round-shaped *Escherichia coli*. *EMBO J.* **21,** 1998–2008
45. Ramirez-Arcos, S., Szeto, J., Dillon, J. A., and Margolin, W. (2002) Conservation of dynamic localization among MinD and MinE orthologues. Oscillation of *Neisseria gonorrhoeae* proteins in *Escherichia coli*. *Mol. Microbiol.* **46,** 493–504
46. Schweizer, J., Loose, M., Bonny, M., Kruse, K., Mönch, I., and Schwille, P. (2012) Geometry sensing by self-organized protein patterns. *Proc. Natl. Acad. Sci. U.S.A.* **109,** 15283–15288
47. Cytrynbaum, E. N., and Marshall, B. D. (2007) A multistranded polymer model explains MinDE dynamics in *E. coli* cell division. *Biophys. J.* **93,** 1134–1150
48. Khalifat, N., Puff, N., Bonneau, S., Fournier, J. B., and Angelova, M. I. (2008) Membrane deformation under local pH gradient. Mimicking mitochondrial cristae dynamics. *Biophys. J.* **95,** 4924–4933
49. Li, G., and Young, K. D. (2012) Isolation and identification of new inner membrane-associated proteins that localize to cell poles in *Escherichia coli*. *Mol. Microbiol.* **84,** 276–295